Spatial and Temporal Dynamics of Urban Green Spaces: An Assessment Using Remote Sensing Time-Series Data in Blantyre City, Malawi

Emmanuel Chinkaka[1*], Hastings Hatton[1], Chikondi Chisenga[1] and Francis Chauluka[2]

[1]Malawi University of Science and Technology,
Department of Earth Sciences, Geo-information Sciences Section,
P.O. Box 5196, Limbe, Malawi

[2]Malawi University of Science and Technology,
Department of Water Resources Management,
P.O. Box 5196, Limbe, Malawi

[*]**Corresponding author Email:** *echinkaka@must.ac.mw*

ABSTRACT

Urban expansion and its ecological footprint are increasing at an alarming rate globally. This is putting pressure on the management of Urban Green Space (UGS) which are vital for biodiversity and ecological conservation. UGS contribute to sustainable development of these urban ecosystems. Recently, UGS have been considered to be substantially important for quality of life. In this study, UGS in the city of Blantyre, which has experienced rapid urbanization from 1990 to 2020, were delineated using remotely sensed Landsat-5 TM and Landsat-8 OLI time-series imagery. Maximum Likelihood Supervised Learning Algorithm was utilized to characterize landcover/landuse (LULC) categories, and further extrapolate to dynamic patterns of Urban Green Spaces (UGS). Kappa statistical coefficient and overall accuracy assessment were used to validate the LULC classification. Post-classification technique was used to compare and empirically categorize LULC and UGS changes between 1990 and 2020. Vector analysis change detection was performed to assess the dynamic patterns in UGS over time. The results indicate rapid decrease in UGS footprint by 19.26km^2 representing a 42% decrease between 1990 and 2020. These changes in the study area are attributed to increased urbanization, population growth, socio-economic development, changes in microclimatic patterns and lack of policy and enforcement by the city authorities. The finding that the UGS in Blantyre city has substantially decreased over the past three decades is significant to the city's policymakers, residents and researchers to better understand the shifting dynamics in LULC, and the particularities of UGS depletion in such a critical city for Malawi's socio-economic growth.

Keywords: *Urban Green Spaces, Ecosystem; Landcover, Landsat, Maximum Likelihood Classifier, Remote Sensing, Change Detection.*

1.0 INTRODUCTION

Urban Green Spaces (UGS) significantly contribute to the sustainable growth of the urban ecosystem and, in a long run, provide a wide range of ecological and social benefits (GarÁon, 2012) . Jin (2013) define UGS as all-natural, semi-natural including artificially vegetated green land that is accessible to the public in urban areas including urban agricultural vegetation cover. Recently, UGS in cities have been considered a vital assert to quality of life, since they have a significant impact on ecosystem functions, local microclimate, air quality, noise absorption and water resources protection (Vatseva *et al.*, 2016). The diversity and quality of urban green spaces such as parks, forests, water bodies, urban agricultural gardens are directly linked to human well-being due to their various ecosystem benefits to the city inhabitants (Kopecká et al., 2017a). Silva et al. (2019) argues that lack of human physical activity is linked to the lack of access to recreational zones and accounts for 3.3% of global deaths. Beside this, environmentally, urban green spaces act as sufficient filter for air pollution and have an impact on moderating intense temperature levels within the cities (Venter et al., 2024). Several factors including anthropogenic activities, have been associated to significant loss and spatial fragmentation of green spaces (Nazombe & Nambazo, 2023). Loss of urban green spaces in many places is significantly attributed to rapid urbanization coupled with human population growth which in-turn drastically affect the landuse and landcover dynamics (Jin, 2013; Nazombe & Nambazo, 2023). *Gondwe et al.* (2021) observed that in Malawi, Blantyre City has experienced a wide range of changes in landuse and landcover due to the interaction between human activities and the environment. Such changes negatively affect human well-being and ecosystem's functions, including increased soil erosion, run-off and flash flooding degrading water quality which may result in spread of water-borne diseases (Liping *et al.*, 2018). Rapid changes and growth in population and infrastructure are directly contributing factors to drastic changes in land use and landcover (LULC) of many cities globally, leading to loss of urban green spaces (Puplampu & Boafo, 2021).

For decades the use of remotely sensed data in conjunction with a geospatial analytical tools has proven to be effective in detecting and monitoring LULC changes in spatial-temporal components (Baig et al., 2022, Chinkaka *et al.*, 2023). In comparison to other conventional methods, remote sensing is a robust, reliable and cost-effective data assessments tool for surface landscape analysis (Baig *et al.*, 2022). The changes in UGS can be monitored through a process that is known as change detection. The method identifies changes in any phenomenon by analyzing time series data (Kumar *et al*., 2008, Pakbaz *et al.*, 2014, Talukdar et al., 2020). When evaluating changes in the spatial features of the land resources, it is important to consider such analysis at multi-temporal, multi-scale and multi-resolution levels

(Gopinath *et al.*, 2014). In landuse/landcover analysis, Supervised Maximum Likelihood Classifier has been used by several researchers. It generates decision based on the mean and covariance of each class in the remotely sensed imagery (Jamali, 2019). Other machine-learning-based algorithms such as artificial neural networks (ANNs), Support Vector Machine, and Random Forest have also been applied for LULC classification and urban green space mapping (Chen *et al*., 2021).

Blantyre City is Malawi's commercial and industrial backbone with a population density of 3,334 people per square kilometer according to the 2018 census (Chinkaka *et al.*, 2023). The city has experienced a tremendous change in LULC during the past decades due to urbanization, an increase in socioeconomic development, and population growth (Gondwe *et al.*, 2021). But not much research has been conducted to establish any multi-temporal changes in the UGS and its relationship to landcover/landuse changes. With Blantyre City experiencing increased urbanization, this lack of research attention and evidence-based policy direction on urban green spaces poses a huge challenge to the realization of sustainable development for city management efforts at spatial planning (Gondwe *et al*., 2021). This study therefore examines the spatial impacts of LULC patterns on the spatial distribution of urban green spaces availability and functional role of providing ecosystem services to urban residents. This was achieved through the analysis of multi-temporal changes in UGS surface extents from 1990 to 2020 using Landsat missions' satellite time series data through landcover change detection. Satellite imagery for 1990, 2000 and 2010 from Landsat 5 TM and 2020 imagery from Landsat 8 Operational Land Imager (OLI) were processed to determine in landcover/landuse, and a change detection analysis was performed to quantify the dynamics of UGS and Non-UGS areas within the city.

1.1 Study Area

The study was undertaken in Blantyre City, located around 15°29′S and 35°00′E in Malawi, with an area of about 240 km^2 (Figure 1). The area was selected for this study owing to its high economic development and the rapid growth of urbanization (Gondwe et al., 2021). It is Malawi's second largest city after Lilongwe and is referred to as Malawi's commercial city. According to the 2018 Malawi Population and Housing Census, the study area had a total population of 800,264 and intercensal growth rate of 2.0 from 2008 (National Statistical Office, 2019). This rapid population increase affects the landuse dynamics which in turn puts pressure on the spatial distribution of urban green spaces in spatial and temporal sense.

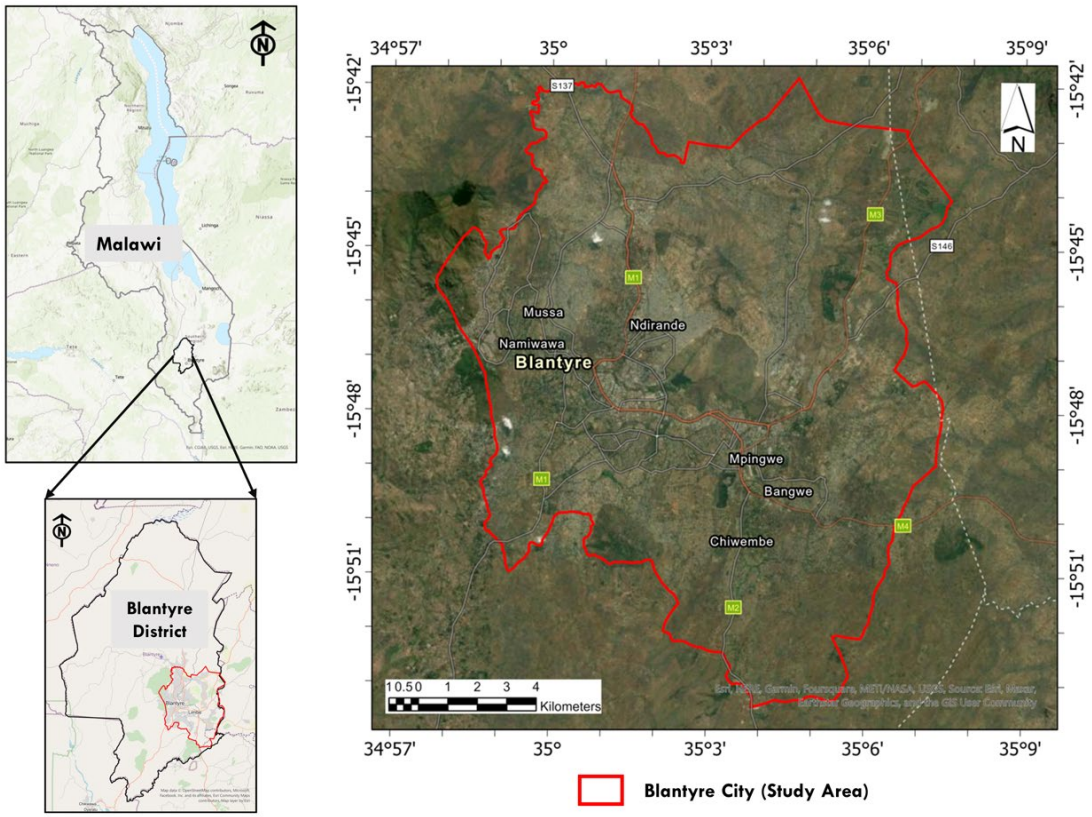

Figure 1: *Location of the study area*

2. Materials and Methods

2.1. Satellite Data and Image Pre-processing

This study utilized three multispectral Landsat 5 Thematic Mapper's (TM) Visible-Near Infrared (VINR), and Shortwave Infrared (SWIR) data, one Landsat 8 Operational Land Imager (OLI) Visible-Near Infrared (VNIR) and Short-Wave Infrared (SWIR) data that were downloaded freely from NASA's Earth data portal through their website (https://search.eartdata.nasa.gov/search, accessed on 15 September 2020) and the administrative vector data shapefile for Malawi that was downloaded freely on http://www.diva-gis.org/, accessed on 20 September 2020. The Landsat 5-TM data comprised of three VNIR-SWIR (Level 1 – surface reflectance) images acquired on three different dates and years and the Landsat 8 OLI comprised of one image of VNIR-SWIR (Level 1 – surface reflectance) data (Table 1). For easy visibility, four cloud free satellite reflectance images were collected over the study between 1990 and 2020 with a 10-year temporal difference.

Table 10: *Satellite Sensor data used*

Satellite Sensor	Date of Acquisition	Path/row	Resolution	Number of Bands
L5 TM	1990/10/08	167/71	30	7
L5 TM	2000/09/01	161/71	30	7
L5 TM	2010/12/18	161/71	30	7
L8 OLI	2020/10/10	161/71	30	9

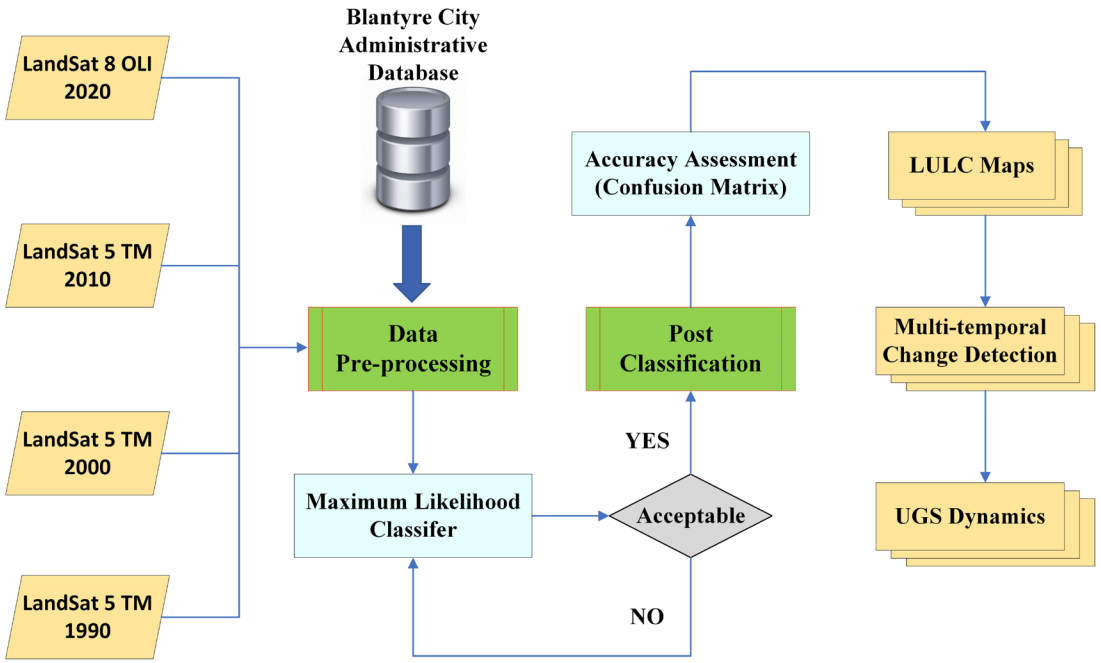

Figure 2: *Research Methodology Workflow*

The satellite images were processed in ENVI 5.3 software through the following links; ENVI 5.3: https://www.nv5geospatialsoftware.com/docs/whatsnew_envi53sp2.html and Maximum likelihood-classifier:

https://www.nv5geospatialsoftware.com/docs/MaximumLikelihood.html. Post-processing steps and geo-visualization of the results were carried out using ArcGIS Pro 2.8. A summarized methodological workflow is illustrated in Figure 2. In this research, image preprocessing techniques were applied to the Landsat time series imagery in order to make them usable for the landcover and landuse mapping, and UGS categorization and change detection. The pre-processing techniques included radiometric, geometric, atmospheric correction and image enhancement through band combinations for visual image interpretation.

To reduce the radiometric errors in the images for the years 1990, 2000, 2010 and 2020, the radiometric correction algorithm in ENVI 5.3 was used to calibrate for all the errors. Radiometric calibration is an automated process of converting the digital number of pixels into spectral radiance values and then radiance into reflectance values (Baig et al., 2022). This process is very important since it improves the interpretability and quality of the multi-temporal remotely sensed data (Kumar *et al.*, 2008). Geometric correction was performed to ensure that the image data are characteristically positioned on the right locations on the surface (Jamali & Abdul Rahman, 2019). This was followed by removing the influence of the atmospheric effects in the images by using the Quick Atmospheric Correction (QUAC) algorithm in-built in ENVI 5.3 environment. The Blantyre City boundary vector data file was used to clip all the satellite images to the city boundary extent.

2.2 Classification Scheme and Sampling for Ground Truthing

A random design technique was utilized to collect a total of 60 field-based points within the city of Blantyre as ground-truthing data for various landuse/landcover categories. Out of these field-based samples, 15 of each belonged to the classes, built-up area, vegetation, bare land and water bodies. Based on (Chinkaka et al., 2023), we utilized a simultaneous visual inspection and interpretation technique of maps generated from Landsat 5TM/8OLI images. These include NDVI maps, Near Infrared False Color Composite, RGB Orthophoto Composite Maps and high-resolution Google Earth imagery to inspect and develop a reliable set of reference labels that were used for model training and accuracy assessment.

2.3 Supervised Maximum Likelihood Classifier

Image classification refers to the task of extracting spectral information classes from a multiband imagery. The resulting raster from this process is normally a thematic map showing the various landcover and landuse categories (Das & Bist, 2015). In this study, Supervised Maximum Likelihood classifier was used to classify the Blantyre city satellite images into four main classes namely built-up areas, vegetation, bare land and water bodies. The set of field-based training samples at a pixel level information was then run in the Maximum Likelihood machine learning oriented classifier algorithm in ENVI 5.3. During the sample training and model

implementation, 70% of the reference labels were used for the model training and the rest for model testing.

Maximum Likelihood is a supervised classification method derived from the Bayes theorem, which utilizes a posteriori distribution P(i|**ω**) (Kumar *et al.*, 2006), which is the probability that a pixel with feature vector ω belongs to class i. It is expressed by:

$$P(i|\boldsymbol{\omega}) = \frac{P(\boldsymbol{\omega}|i)\,P(i)}{P(\boldsymbol{\omega})} \quad (1)$$

where P(ω|i) is the likelihood function, P(i) is the priori information, i.e., the probability that class i occurs in the study area and P(ω) is the probability that ω is observed, which can be written as:

$$P(\boldsymbol{\omega}) = \sum_{i=1}^{M} P(\omega|i)\,P(i) \quad (2)$$

And M is the number of classes. P(**ω**) is often treated as a normalization constant to ensure $\sum_{i=1}^{M} P(i|\omega)$ sums up to 1. Pixel x is assigned to class i by the rule:

$x \in i$ if $P(i|\omega) > P(j|\omega)$ for all $j \neq I$, (3)

The Maximum Likelihood Algorithm usually assumes that the distribution of the data within a given class i and follows a multivariate Gaussian distribution (Kumar *et al.*, 2011, Pakbaz *et al.*, 2014, Talukdar *et al.*, 2020). Because of this assumption, it is then imperative to define the log likelihood as follows:

$$g_i(\boldsymbol{\omega}) = \mathrm{In}P(\omega|i) = -\frac{1}{2}(\omega - \mu_i)^t C_i^{-1}(\omega - \mu_i) - \frac{N}{2}\mathrm{In}(2\pi) - \frac{1}{2}\mathrm{In}(|\,C_i\,|), \quad (4)$$

Since log is a monotonic function, Equation (3) is then equivalent to:

$x \in i$ if $g_i(\omega) > g_j(\omega)$ for all $j \neq i$. (5)

2.3.1 Accuracy Validation

Accuracy assessment is essential in remote sensing-based research since decision making with data of unknown or little accuracy has the potential to misclassify the satellite data. If the reference data has information with low reliability, the accuracy is affected (Chinkaka *et al.*, 2023). We performed an accuracy assessment of the classified images using confusion matrix analysis. This approach demonstrates the accuracy of a classified result by comparing it to the ground-based reference data (Munthali *et al.*, 2019). Overall Accuracy (OA) and Cohen's Kappa Coefficient (k) in a confusion matrix analysis (de Raadt *et al.*, 2021, Więckowska *et al.*, 2022) were used to assess the validity of the classification results as follows:

$$k = \frac{N\sum_{i=1}^{n} m_{i,i} - \sum_{i=1}^{n}(C_i G_i)}{(N^2 - \sum_{i=1}^{n}(C_1 G_i)} \quad (6)$$

where *i* stands for the class number, *N*, denotes the total number of classified pixels with respect to the field data, $m_{i,i}$ representing the number of pixels of field data class *i*, which have been assigned to class *i*, *Ci* is representing the total number of classified pixels in class *i*, and *Gi* denoting the total number of field data pixels in class *i.*

In this study, a total of 60 test pixels for all landcover classes were collected for each separate image and were used to perform the accuracy assessment of each classification result (He & Garcia, 2009). Thus, agreement and disagreement of the analysis was evaluated by using an error matrix and simple descriptive statistics based on (Zhai *et al*., 2021).

2.4 Categorization of landcover into Urban Green Spaces (UGS)

The four landcover classes: built-up area, vegetation, bare land and water bodies were further processed and categorized into urban green spaces pixels and non-urban green spaces pixels. This categorization is based on research by (Vatseva *et al*., 2016). As such, vegetation and water bodies classes were categorized as urban green spaces and built-up Area and bare land were categorized as non-urban green spaces (Table 2).

Table 11: *Categorization criteria of the landuse-landcover classes and UGS and Non-UGS*

Landcover class	Description	Category
Built-up Area	Consists of Urban, Industrial, commercial, and transport units, dump, and construction sites	Non-UGS
Bare land	Spaces with little or no vegetation, beaches, dunes sands, bare rocks, sparsely vegetated areas	Non-UGS
Vegetation	Urban forests, Shrub and herbaceous vegetation association, Urban recreation centers, Parks, Permanent crops, Pastures, and Heterogeneous urban agricultural areas.	UGS
Water Bodies	Watercourses, dam areas	UGS

2.5 UGS and Non-UGS Change Detection

A UGS and Non-UGS change matrix from the initial year of analysis (1990) to the final year of analysis (2020) were computed based on cumulative classified maps. We generated an evaluation of gains and losses, net change, persistence, and specific transitions (Meier & Mauser, 2023; Zhang et al., 2022). Based on the principle of land change analysis, geo-visualization maps of gains and losses of UGS and Non-UGS were generated to quantify the changes in space and time (Panuju et al., 2020). The area changes of the UGS and Non-UGS categories are a result of the post-classification, which corresponds to the area unit covered by category pixels (Chinkaka *et al*., 2023). And change detection statistics was used to compile a detailed tabulation of changes between images acquired between a period of 1990 and 2020.

3. RESULTS

3.1. LULC Analysis Distribution Pattern

The Maximum likelihood Algorithm classification of the four Landsat images resulted in LULC thematic maps for each year (Figure 3) showing the spatial distribution of four classes in the study area. Figure 4 shows the area statistical distribution of LULC and their percentage coverage for each year based on the classification results.

The classification findings indicate that the bare land class is most dominant in the study area. It occupied an area of 163.89km^2, 160.81km^2, 157.58km^2 and 137.69km^2 in the years 1990, 2000, 2010 and 2020 respectively accounting for 68.13%, 66.85%, 65.51% and 57.24% of the total area cover. From this analysis, it shows that the bare land class has been reducing in area coverage over the years. Vegetation class was detected as the second largest class only for the years 1990 and 2000 with a total area coverage of 45.36km^2 and 40.11km^2 representing 18.86% and 16.67% respectively. But for the years 2010 and 2020, vegetation class has drastically reduced and become the third largest class in the city with a total area coverage of 32.78km^2 and 26.20km^2 accounting for 13.63% and 10.89% respectively. The built-up class was the third largest class between the years 1990 and 2000 with area coverage of 30.96km^2 and 39.34km^2 representing 12.96% and 16.36% respectively. But in the years 2010 and 2020 the built-up area class has rapidly increased and became the second largest class with spatial statistical area coverage of 49.94km^2 and 76.43km^2 accounting for 20.76% and 31.77% increase respectively. And lastly, the water bodies class has been the lowest class and been decreasing rapidly in area size throughout the years 1990. 2000, 2010 and 2020 with a coverage of 0.33km^2, 0.28km^2, 0.25km^2 and 0.23km^2 representing 0,14%, 0.12%, 0,10% and 0.10% respectively (Figure 4).

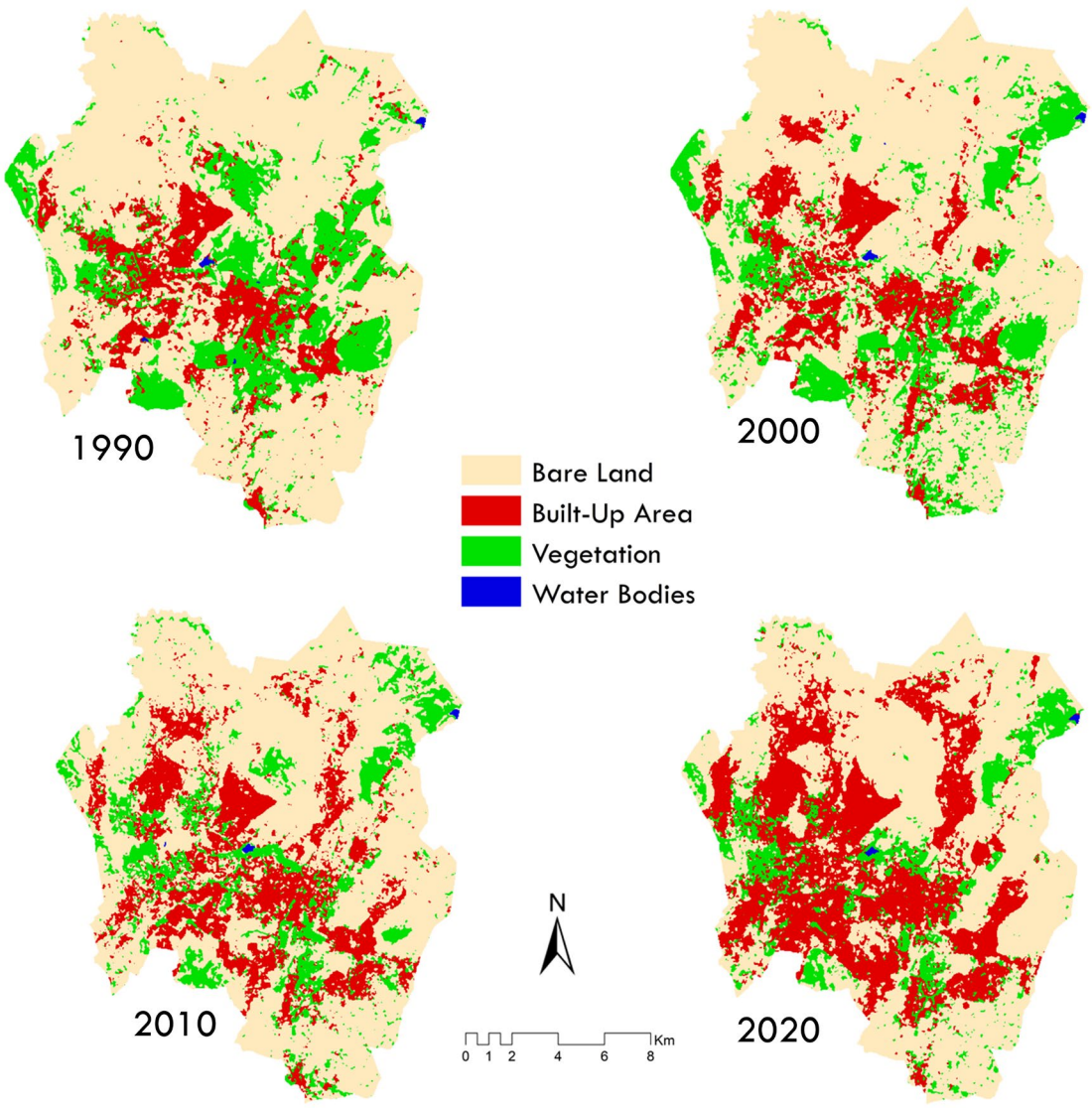

Figure 3: *LULC maps of Landsat-5 and Landsat-8 images for the year 1990, 2000, 2010 and 2020*

Accuracy assessments for the 1990, 2000, 2010 and 2020 images indicated an average overall accuracy of 91% and a Kappa Coefficient of 0.88. According to Baig *et al.* (2022), this is a good result since the overall accuracy for all the classified maps were above 85%. A confusion matrix in Table 3 indicates the user's and producer's accuracies for the given individual landcover/landuse classes for each thematic classified map for each year.

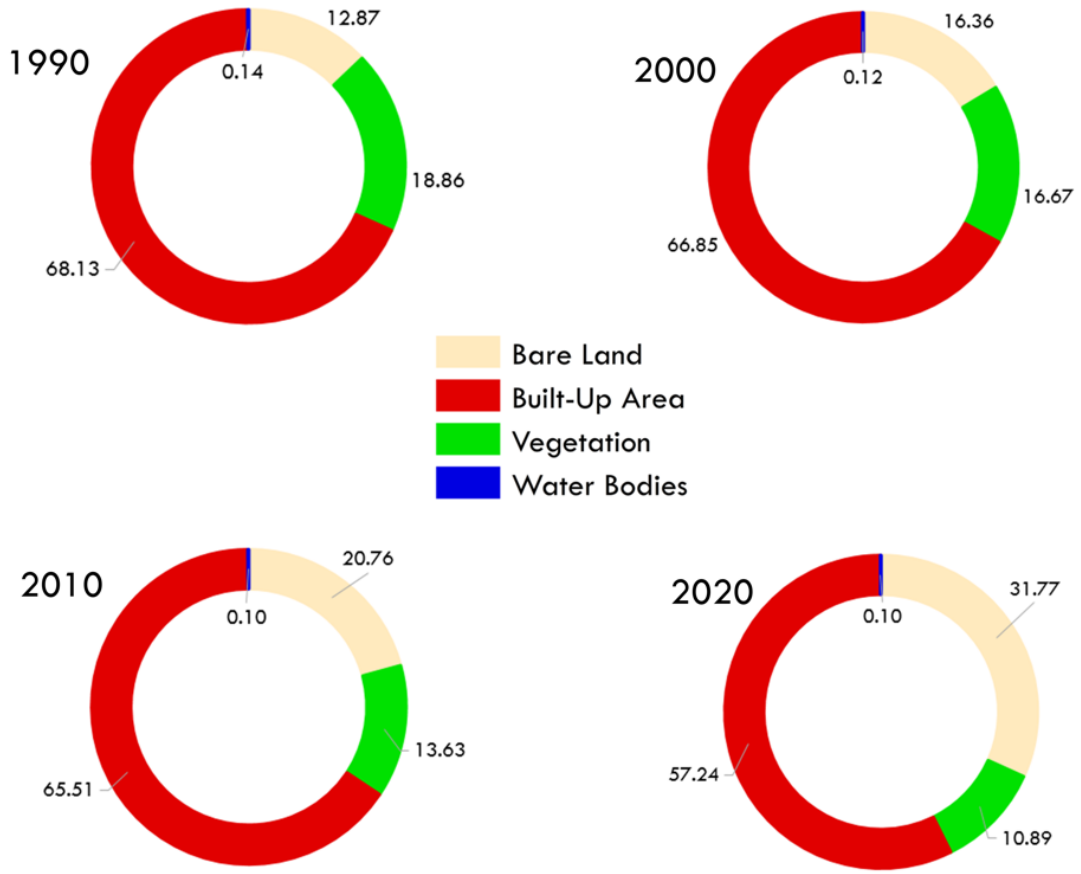

Figure 4: *Area statistics in LULC changes for the years 1990, 2000, 2010 and 2020*

Table 12: *Confusion Matric for the accuracy assessment for classified thematic maps (1990, 2000, 2010, and 2020)*

LULC Class	Built-up Area	Vegetation	Water Bodies	Bare land	Total	User's Accuracy (%)
1990						
Built-up Area	15	0	0	3	18	83.33
Vegetation	0	15	0	0	15	100
Water bodies	0	0	15	0	15	100
Bare land	0	0	0	12	12	100
Total	15	15	15	15	60	
Producer's Accuracy (%)	100	100	100	80		
Overall Accuracy (%)	95					

LULC Class	Built-up Area	Vegetation	Water Bodies	Bare land	Total	User's Accuracy (%)
Kappa Coefficient	0.933					
2000						
Built-up Area	15	1	0	5	21	71.43
Vegetation	0	14	3	0	17	82.35
Water bodies	0	0	12	0	12	100
Bare land	0	0	0	10	10	100
Total	15	15	15	15	60	
Producer's Accuracy (%)	100	93.33	80	66.67		
Overall Accuracy (%)	85					
Kappa Coefficient	0.8					
2010						
Built-up Area	13	0	0	2	15	86.67
Vegetation	1	15	0	1	17	88.24
Water bodies	0	0	15	0	15	100
Bare land	1	0	0	12	13	92.31
Total	15	15	15	15	60	
Producer's Accuracy (%)	86.67	100	100	80		
Overall Accuracy (%)	93.33					
Kappa Coefficient	0.91					
2020						
Built-up Area	15	0	0	3	18	83.33
Vegetation	0	15	0	1	16	93.75
Water bodies	0	0	15	0	15	100
Bare land	0	0	0	11	11	100
Total	15	15	15	15	60	
Producer's Accuracy (%)	100	100	100	73.33		
Overall Accuracy (%)	91.67					
Kappa Coefficient	0.88					

3.2. UGS – Non-UGS Classification

The classified LULC maps for all the four years were further post-processed into two categories of UGS class and Non-UGS class. The post-processing findings indicate that in all the four images, Non-UGS class is dominant in the study area. It occupied an area of 194.85km^2, 200.15km^2, 207.52km^2 and 214.11km^2 in the years 1990, 2000, 2010 and 2020 respectively accounting for 81%, 83.21%, 86.27% and 89.01% of the total spatial area cover (Figure 5). This indicates that the UGS Category has been reducing drastically from 1990, 2000, 2010 and 2020 with the area coverage of 45.70 km^2, 40.39km^2, 33.03km^2 and 26.43km^2 respectively. Between 1990 and 2020 the UGS category has drastically reduced with an average of 36.50%. This is a huge reduction to the urban green spaces in the city, which in-turn reduces the biodiversity functionalities in the city. The spatial dynamic distribution of UGS and Non-UGS in Blantyre city is depicted in Figure 6.

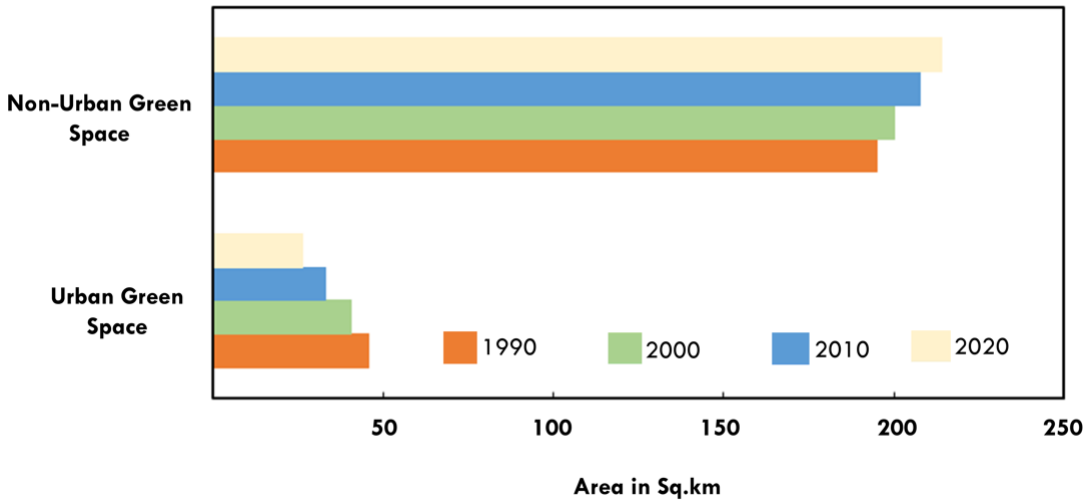

Figure 5: *UGS and Non-UGS changes based on Landsat-5 and Landsat-8 for the years 2005, 2010, 2015, and 2020*

3.3. Urban Green Space Trajectory Dynamics

The post classification and categorization comparison change detection analysis results show that urban green space has rapidly changed in the study area over the last three decades. Table 6 shows the change matrix that has occurred of the last three decades. It stipulates the amount and type of change that has occurred between urban green spaces and none-urban green spaces classes.

The change matrix and corresponding statistics from 1990, 2000, 2010 and 2020 were modeled using the categorization of the urban green space and non-urban green space cover based on the landcover and land use classifications for each year. The analysis focused primarily on the initial state classification changes; that is, for each initial state class, the analysis identifies the classes into which, those pixels changed in the final state image. The change matrix (Table 4) gives an account of the transitions in changes of urban green spaces and non-urban green spaces classes between 1990 and 2020.

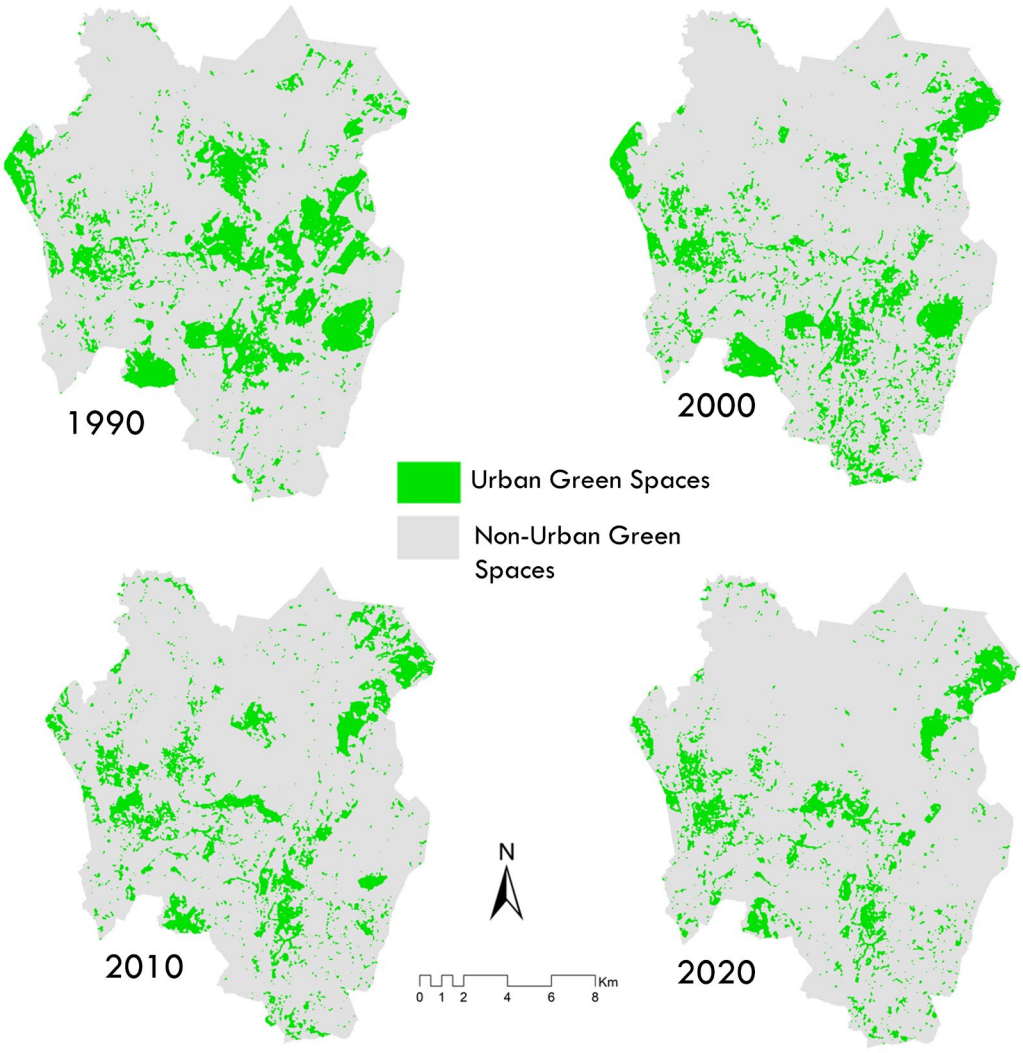

Figure 6: *Spatial distribution of urban green spaces and Non-Urban Green Spaces in 1990, 2000, 2010 and 2020*

The "Class Total" row shows the total surface area in square kilometers (km^2) in each initial and final state class. The "Image Difference" row shows how a class has either grown or shrunken whereby positive values mean to gain and negative values mean loss. From the table above there has been a loss in green spaces, over the past three decades, a total surface area of $19.26.72km^2$ for urban green spaces has been lost. Table 4 shows that there has been tremendous growth in the non-urban green spaces by $19.2672km^2$. Figure 7 depicts the spatial models of the change detection analysis for 1990 to 2000, 2000 to 2010, 2010 to 2020 and an overall change detection showing change to urban green spaces for 1990 to 2020.

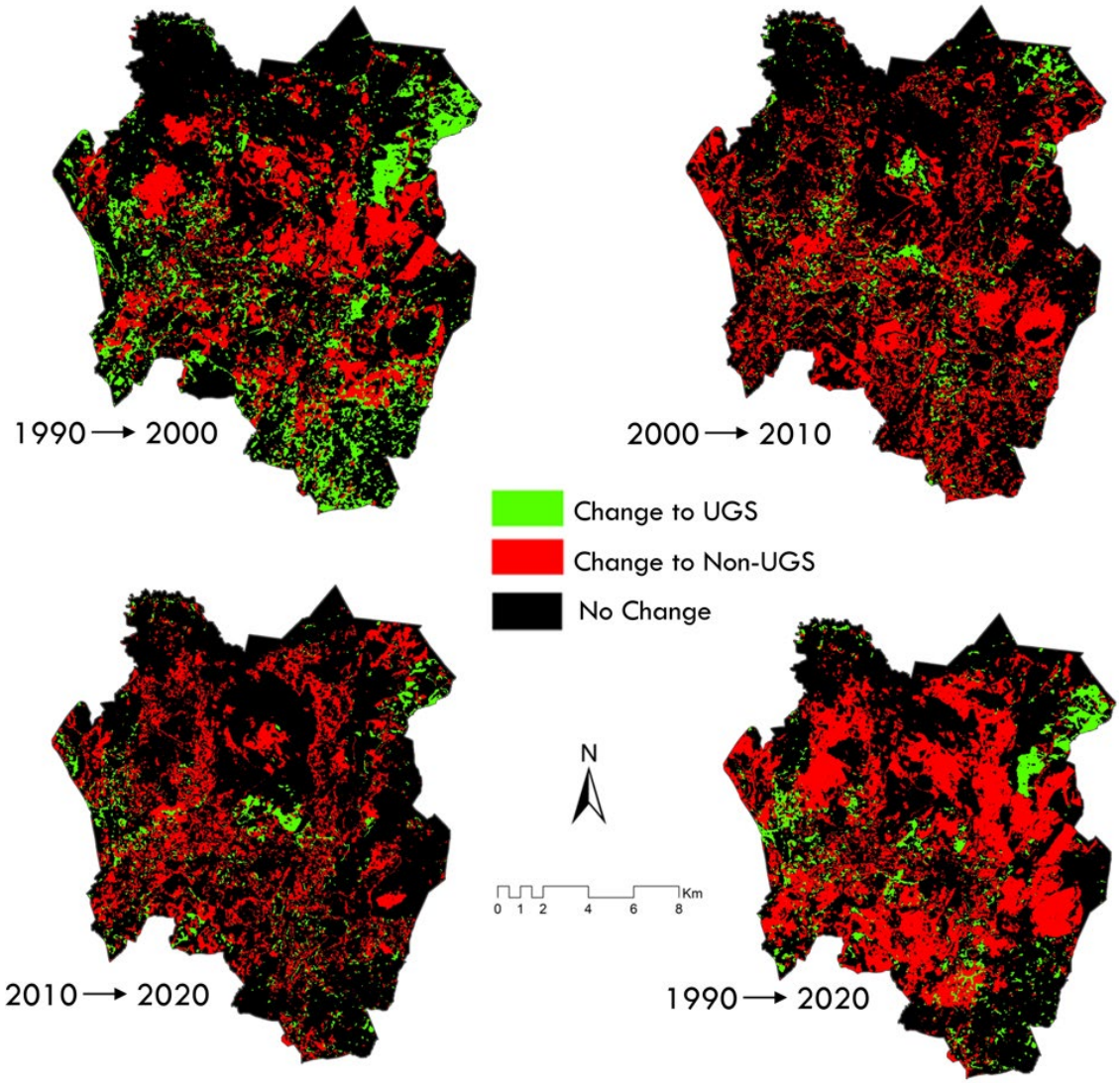

Figure 7: *Change detection maps of urban green spaces for 1990 to 2000, 2000 to 2010, 2010 to 2020 and overall change detection for 1990 to 2020.*

4. DISCUSSION

Based on the results from this study, it has been revealed that Blantyre City has undergone massive LULC change as indicated by the confusion matrix for the post classification analysis. The built-up area class has rapidly increased by 146.87% between 1990 and 2020. This increase is attributed to population increase due to

Table 13: *Category/Class transitions from the initial state (1990) to the final state (2020)*

	Initial State (1990)			
	Category/Class	Green Spaces	Non-Green Spaces	Class Total
Final State (2020) (2020)	Urban Green Spaces	11.89	14.61	26.4303
	None- Urban Green Spaces	33.88	19.2672	214.1127
	Class Total	45.6975	194.8455	
	Image Difference	-19.2672	19.2672	

urbanization subsequently leading to significant reduction in UGS in the city. Reduction of UGS areas by 42.16% in the past three decades is associated to increased urbanization depicted by rapid expansion of the building footprint in the city over the year.

Urban green spaces being public spaces, are supposed to be regulated by the policy and regulations of the city council or other state agencies. As such this reduction is a contribution of the lack of enforcement and policy guidance. Due to this, there has been more built-up area development in these urban green spaces leading to informal settlements within the city. This urban and unplanned settlement structures result in emerging of various negative health related impacts in the city such as malaria, diarrhea and cholera (Gordon, 2001, M'bangombe *et al.*, 2018). According to Malawi Housing Population Census of 2018, Blantyre city shows an increase in population of 23.34% between 2008 and 2018, because of this increase the non-urban green spaces increased drastically from an area spatial value of 194.84km^2 to 214.11Km^2 accounting for an increase from 81% to 89.01% respectively in 1990 and 2020. Another critical contributor to the increased non-urban green space is the increased socio-economic growth of the population. This involved the clearing of vegetative space for construction of various built-up areas for settlement and economic ventures. However, this can be controlled better by the policy support from the city council in environmental management of the urban green space which is a very important component of the ecosystem functions and biodiversity increase

(Rakhshandehroo *et al.*, 2017). Water bodies are among the most important UGS classes that provide the most benefits to the inhabitants and the functionalities of the ecosystem (Bowler et al., 2010, Rakhshandehroo *et al.*, 2017). The water bodies class in the study area has reduced from 0.33km^2 in 1990 to 0.23km^2 in 2020 representing 30% reduction on space. Water bodies are important as habitants of aquatic life in the city. This poses a threat to quality of life since water is one of the basic needs of life for humans, animals and plants which are essential to biodiversity balance in the ecosystem (Rouquette *et al.*, 2013).

The analysis of this study focused primarily on the initial state (1990) classification changes; that is, for each initial state class, the analysis identifies the classes into which those pixels changed in the final state image (2020). As visualized in Figure 7, the transitions of UGS and None-UGS classes between 1990 and 2020, indicates the spatial distribution through post-classification a vector change detection analysis. It shows that there has been a depletion of UGS in the southern part of the city transitioning to None-UGS in 1990 and 2020 respectively. This drastic three-decade decrease in UGS (Table 4) with about 19.26Km^2 of UGS has transitioned to None-UGS areas. And none of the Non-UGS areas have transitioned to UGS areas, this shows that not even the bare-lands are being developed into UGS areas. This means that only the UGS areas have been declining in the city. Based on this, Blantyre City has seen a remarkable increase in built-up areas and a decrease in undeveloped territory such as bare land. This indicates that various natural forests and habitats have been deforested, resulting in the conversion of previously green landscapes into non-green ones. Therefore, this drastic decline of UGS will results into pressure on water resources in the city, not only due to decline in water bodies but also because of increase in population growth and urbanization. These two have a direct negative impact on the ecosystem landscape. Further to this, the reduced UGS shall result into improper balance of the rainfall and temperature intensities in the city, causing increased dry spells. This is consistent with the findings of (Gondwe et al., 2021) who revealed using climate data that the study area has been experiencing occasional dry spells in which the amount of rainfall received decreased significantly between 1990 to 2019. Further to this, the reduced UGS impacts negatively on the biodiversity as it reduces the habitats of most wildlife both aquatic and terrestrial species that are normally found with the urban perimeters. The loss of such ecosystem functions in-turn affects the quality of air and life since UGS are utilized as recreation centers for wellbeing improvement through physical exercise, reducing the need to treat for anxiety and mental health conditions (Soininen et al., 2007) .

5. CONCLUSION

The present study has identified changes in LULC and UGS patterns in the commercial city of Blantyre from 1990 to 2020 using Landsat 5 TM and Landsat 8

OLI time-series imagery. In combination with LULC field-based sampling, a machine learning-powered multi-temporal change detection analysis was performed to assess the LULC and UGS dynamics in the study area. Maximum Likelihood Classifier algorithm was employed to determine the LULC dynamics with four main classes (built-up area, bare land, and vegetation and water bodies). Our results showed that urban green spaces in the city of Blantyre has experienced loss and dynamic fragmentation with depletion of urban green spaces transitioning to non-urban green space with a decrease of 19.26Km^2 between 1990 and 2020. This is significantly a huge change in LULC where the built-up areas have increased with 146.87% between 1990 and 2020. This increase is due to urbanization, increased socio-economic growth and population increase. Such information is crucial to understanding the transformation processes and human–environment with the growing city population. The increase in built-up areas has also resulted in reduction of green spaces since people have transitioned urban green spaces into settlements (built-up areas). Among the factors that have led to this reduction include lack of enforcement of urban green spaces conservation, poor planning and policy implementation strategies. Most urban green spaces such as vegetated parks and forests have been depleted due to increased demand for timber, and charcoal as a source of energy in the peri-urban wards within the city (Gondwe *et al.*, 2021). Additionally, the decrease in the water bodies is attributed to changes in microclimate and siltation in the dams resulting in the reduction of the spatial area size of the dams. The presence of urban green spaces is beneficial to the city residents in such a way that they provide quality health and wellbeing, regulates temperature levels and climate, provides good quality air and act as habitats for various wildlife and restores the ecosystem. Therefore, a better understanding of LULC dynamics and urban green spaces patterns is critical to the realization of the high standard of living and quality of life, and increasing accessibility to green public spaces as outlined in the African Union's Agenda for 2063 and United Nation's Sustainable Development Goals 2030.

6. AUTHOR CONTRIBUTIONS

The authors would like to thank Malawi University of Science and Technology and the United States Geological Survey for the freely available Landsat satellite data that was used in this study.

Emmanuel Chinkaka: Conceptualization, Data analysis, post-processing analysis, Drafting, Map Design **Hastings Hatton**: Data analysis, Data Pre-processing, **Chikondi Chisenga:** Reviewing, Editing, **Francis Chauluka:** Reviewing, Editing.

7. FUNDING

This research did not receive any funding.

8. DECLARATION OF CONFLICT OF INTEREST

The authors declare that they have no known competing financial interests or personal relationships that could have appeared to influence the work reported in this paper.

9. REFERENCES

Baig, M. F., Mustafa, M. R. U., Baig, I., Takaijudin, H. B. & Zeshan, M. T. (2022). Assessment of Land Use Land Cover Changes and Future Predictions Using CA-ANN Simulation for Selangor, Malaysia. *Water (Switzerland)*. 14(3). https://doi.org/10.3390/w14030402

Bowler, D. E., Buyung-Ali, L., Knight, T. M. & Pullin, A. S. (2010). Urban greening to cool towns and cities: A systematic review of the empirical evidence. *Landscape and Urban Planning* 97(3):147–155. https://doi.org/10.1016/j.landurbplan.2010.05.006

Chen, Y., Weng, Q., Tang, L., Liu, Q., Zhang, X. & Bilal, M. (2021). Automatic mapping of urban green spaces using a geospatial neural network. *GIScience & Remote Sensing*, *58*(4), 624–642. https://doi.org/10.1080/15481603.2021.1933367

Chinkaka, E., Davis, K. F., Chiwanda, D., Kachingwe, B., Gusala, S., Mvula, R., Chauluka, F. & Klinger, J. M. (2023). Geospatial Coronavirus Vulnerability Regression Modelling for Malawi Based on Cumulative Spatial Data from April 2020 to May 2021. *Journal of Geographic Information System* 15(01):110–121. https://doi.org/10.4236/jgis.2023.151007

Chinkaka, E., Klinger, J. M., Davis, K. F. & Bianco, F. (2023). Unexpected Expansion of Rare-Earth Element Mining Activities in the Myanmar–China Border Region. *Remote Sensing* 15(18) Article 18. https://doi.org/10.3390/rs15184597

Das, P. & Bist, A. (2015). *Image Classification 4*(2):202–204.

de Raadt, A., Warrens, M. J., Bosker, R. J. & Kiers, H. A. L. (2021). A Comparison of Reliability Coefficients for Ordinal Rating Scales. *Journal of Classification* 38(3):519–543. https://doi.org/10.1007/s00357-021-09386-5

GarÁon, P. (2012). Jardin des plantes. *European Green Capital Award Nantes*.

Gondwe, J. F., Lin, S. & Munthali, R. M. (2021). Analysis of Land Use and Land Cover Changes in Urban Areas Using Remote Sensing: Case of Blantyre City. *Discrete Dynamics in Nature and Society* 1–17. https://doi.org/10.1155/2021/8011565

Gopinath, R., Akella, V. & Bhanumurthy, P. (2014). *Comparison studies in Landcover Mapping Analysis*. https://www.semanticscholar.org/paper/Comparison-studies-in-Landcover-Mapping-Analysis-Gopinath-Akella/bccd8644f5a6d033b96149de7621bde65b856c40

Gordon, M. (2001). Three Cases of Bacteremia Caused by Vibrio cholerae O1 in Blantyre, Malawi. *Emerging Infectious Diseases* 7(6):1059–1061. https://doi.org/10.3201/eid0706.010629

He, H., & Garcia, E. A. (2009). Learning from Imbalanced Data. *IEEE Transactions on Knowledge and Data Engineering* 21(9):1263–1284. https://doi.org/10.1109/TKDE.2008.239

Jamali, A. (2019). Evaluation and comparison of eight machine learning models in land use/land cover mapping using Landsat 8 OLI: A case study of the northern region of Iran. *SN Applied Sciences*, *1*(11), 1448. https://doi.org/10.1007/s42452-019-1527-8

Jamali, A. & Abdul Rahman, A. (2019). Evaluation of Advanced Data Mining Algorithms in Land Use/Land Cover Mapping. *The International Archives of the Photogrammetry, Remote Sensing and Spatial Information Sciences*, *XLII-4/W16*, 283–289. https://doi.org/10.5194/isprs-archives-XLII-4-W16-283-2019

Jin, W. (2013). A MSPA-based Planning of Urban Green Infrastructure Network——A Case of Shenzhen. *Chinese Landscape Architecture*. https://www.semanticscholar.org/paper/A-MSPA-based-Planning-of-Urban-Green-Infrastructure-Jin/180c65764a097ea285e2f84ff07311fc7cd2eb06

Kopecká, M., Szatmári, D. & Rosina, K. (2017a). Analysis of Urban Green Spaces Based on Sentinel-2A: Case Studies from Slovakia. *Land* 6(2):2. https://doi.org/10.3390/land6020025

Kopecká, M., Szatmári, D. & Rosina, K. (2017b). Analysis of urban green spaces based on sentinel-2A: Case studies from Slovakia†. *Land*,*6*(2). https://doi.org/10.3390/land6020025

Kumar, U., Kerle, N., Atzberger, C. & Punia, M. (2008). Evaluation of Algorithms for Land Cover Analysis using Hyperspectral Data. *Indian Space Research Organization – Indian Institute of Science – Space Technology Cell (ISRO – IISc – STC)* 1.

Kumar, U., Kerle, N. & Punia, M. (2011). Mining Land Cover Information Using Multilayer Perceptron and Decision Tree from MODIS Data. *Indian Society*

of Remote Sensing. 38 (4):592-603. https://doi.org/10.1007/s12524-011-0061-yhttps://doi.org/10.1007/s12524-011-0061-y.

Kumar, U., Ramachandra, T. V., Kerle, N., Atzberger, C. & Punia, M. (2006). Evaluation of Algorithms for Land Cover Analysis using Hyperspectral Data Address for Correspondence. *Technical Report 111*.

Liping, C., Yujun, S. & Saeed, S. (2018). Monitoring and predicting land use and land cover changes using remote sensing and GIS techniques—A case study of a hilly area, Jiangle, China. *PLOS ONE* 13(7):e0200493. https://doi.org/10.1371/journal.pone.0200493

M'bangombe, M., Pezzoli, L., Reeder, B., Kabuluzi, S., Msyamboza, K., Masuku, H., Ngwira, B., Cavailler, P., Grandesso, F., Palomares, A., Beck, N., Shaffer, A., MacDonald, E., Senbete, M., Lessler, J., Moore, S. M. & Azman, A. S. (2018). Oral cholera vaccine in cholera prevention and control, Malawi. *Bulletin of the World Health Organization* 96(6):428–435. https://doi.org/10.2471/BLT.17.207175

Meier, J. & Mauser, W. (2023). Irrigation Mapping at Different Spatial Scales: Areal Change with Resolution Explained by Landscape Metrics. *Remote Sensing* 15:315. https://doi.org/10.3390/rs15020315

Munthali, M. G., Botai, J. O., Davis, N. & Adeola, A. M. (2019). Multi-temporal Analysis of Land Use and Land Cover Change Detection for Dedza District of Malawi using Geospatial Techniques. *International Journal of Applied Engineering Research*, *14*(5), 1151–1162.

National Statistical Office. (2019, June 10). *Malawi 2018 Population and Housing Census Main Report*. UNFPA Malawi. https://malawi.unfpa.org/en/resources/malawi-2018-population-and-housing-census-main-report

Nazombe, K. & Nambazo, O. (2023). Monitoring and assessment of urban green space loss and fragmentation using remote sensing data in the four cities of Malawi from 1986 to 2021. *Scientific African* 20:e01639. https://doi.org/10.1016/j.sciaf.2023.e01639

Pakbaz, N., Fathizad, H., Tazeh, M., & Yosefi, A. (2014). Investigating the process of landuse agriculture changes in Dasht – e- Akbar region via artificial neural network and satellite images. *International Journal of Agriculture and Crop Sciences*.

Panuju, D., Paull, D. & Griffin, A. (2020). Change Detection Techniques Based on Multispectral Images for Investigating Land Cover Dynamics. *Remote Sensing* 12:1781. https://doi.org/10.3390/rs12111781

Puplampu, D. A. & Boafo, Y. A. (2021). Exploring the impacts of urban expansion on green spaces availability and delivery of ecosystem services in the Accra metropolis. *Environmental Challenges* 5:100283. https://doi.org/10.1016/j.envc.2021.100283

Rakhshandehroo, M., Mohd Yusof, M. J., Arabi, R., Parva, M. & Nochian, A. (2017). The environmental benefits of urban open green spaces. *ALAM CIPTA, International Journal on Sustainable Tropical Design Research & Practice* 10(1):1.

Rouquette, J. R., Dallimer, M., Armsworth, P. R., Gaston, K. J., Maltby, L. & Warren, P. H. (2013). Species turnover and geographic distance in an urban river network. *Diversity and Distributions* 19(11):1429–1439. https://doi.org/10.1111/ddi.12120

Silva, D. A. S., Naghavi, M., Duncan, B. B., Schmidt, M. I., de Souza, M. de F. M. & Malta, D. C. (2019). Physical inactivity as risk factor for mortality by diabetes mellitus in Brazil in 1990, 2006, and 2016. *Diabetology & Metabolic Syndrome* 11:23.

https://doi.org/10.1186/s13098-019-0419-9

Soininen, J., Lennon, J. J. & Hillebrand, H. (2007). A multivariate analysis of beta diversity across organisms and environments. *Ecology* 88(11):2830–2838. https://doi.org/10.1890/06-1730.1

Talukdar, S., Singha, P., Mahato, S. & Pal, S. (2020). Land-Use Land-Cover Classification by Machine Learning Classifiers for Satellite Observations—A Review. *Remote Sensing*. https://doi.org/10.3390/rs12071135

Vatseva, R., Kopecka, M., Otahel, J., Rosina, K., Kitev, A., Genchev Rumiana Vatseva, S. & Genchev, S. (2016). Mapping urban green spaces based on remote sensing data: Case studies in Bulgaria and Slovakia. *Proceedings, 6th International Conference on Cartography and GIS* 3–17.

Venter, Z. S., Hassani, A., Stange, E., Schneider, P. & Castell, N. (2024). Reassessing the role of urban green space in air pollution control. *Proceedings of the National Academy of Sciences of the United States of America* 121(6):e2306200121. https://doi.org/10.1073/pnas.2306200121

Więckowska, B., Kubiak, K. B., Jóźwiak, P., Moryson, W. & Stawińska-Witoszyńska, B. (2022). Cohen's Kappa Coefficient as a Measure to Assess

Classification Improvement following the Addition of a New Marker to a Regression Model. *International Journal of Environmental Research and Public Health* 19(16):16. https://doi.org/10.3390/ijerph191610213

Zhai, H., Lv, C., Liu, W., Yang, C., Fan, D., Wang, Z. & Guan, Q. (2021). Understanding Spatio-Temporal Patterns of Land Use/Land Cover Change under Urbanization in Wuhan, China, 2000–2019. *Remote Sensing* 13(1): 16. https://doi.org/10.3390/rs13163331

Zhang, C., Dong, J., Zuo, L. & Ge, Q. (2022). Tracking spatiotemporal dynamics of irrigated croplands in China from 2000 to 2019 through the synergy of remote sensing, statistics, and historical irrigation datasets. *Agricultural Water Management* 263:07458. https://doi.org/10.1016/j.agwat.2022.107458